Chapter 3

Magnetic domain theory in dynamics

Microscale magnetization reversal dynamics is one of the hot issues, because of a great demand for fast response and high density data storage devices, for example SV and MTJ systems. Such devices are operating in the ns regime, where magnetization reversal takes place by magnetic domain nucleation and domain wall propagation (see Fig. 1.3). In this chapter, the mechanism of the magnetic domain wall motion in the ns range and slower will be explained.

In Fig. 3.1, the relation between velocity of wall motion and magnetic field is schematically shown. In the low field range, the velocity increases exponentially with field. The wall motion in this range is so called thermally activated motion (Section 3.1). Upon increasing the field, the velocity comes into a regime linear with field, viscous wall motion (Section 3.2). Extrapolation of this linear part to the field axis is called the critical field, H_{Crit}, which is about a border between these two regimes. The velocity does not increase infinitely, but saturates at some field, the so

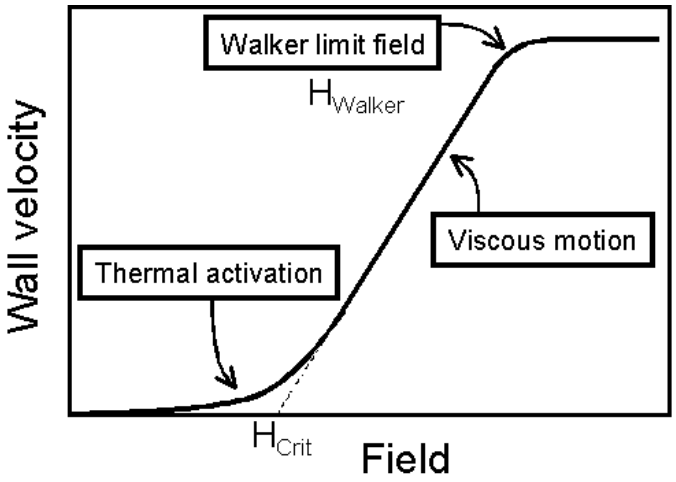

Figure 3.1: The relation between velocity of wall motion and magnetic field in thermally activated motion, in viscous motion and above the Walker limit field.

called Walker limit field, H_{Walker}, (Section 3.3). Above H_{Walker}, the velocity may fluctuate and/or even oscillate as a function of field.

3.1 Thermally activated wall motion

By quasi-static magneto optical Kerr effect (MOKE) measurements, square-shaped hysteresis loop will be obtained along the easy axis of magnetization. A typical loop is drawn in Fig. 3.2. The squared loop indicates that the magnetization reversal starts at the intrinsic surface defects or the edge of the specimen where domains are nucleated, and the walls propagate. However, if one looks at the hysteresis loop closely, one could see that it is making a step-like behavior (inset in Fig. 3.2). This means that the domain walls proceed in a step-by-step motion. The wall motion is hindered/pinned by surface defects, such as grain boundaries, surface roughness and/or large crystalline imperfections [11, 41]. When the external field, H, is lower than the coercivity, H_C, the domain walls proceed by successive thermally activated jumps. Magnetization reversal by thermally activated domain wall motion has been widely investigated [8–11, 41–44]. Fatuzzo [45] has proposed the mechanism of domain wall propagation in ferroelectrics, which was extended to the magnetic domain wall motion in magnetics by Labrune [9]. The speed of wall motion can be described by following equation,

$$\mathrm{v} = \mathrm{v}_0 \exp\left(\frac{\mu_0 M_S H \mathrm{V_B} - \mathrm{E_P}}{k_B T}\right), \tag{3.1}$$

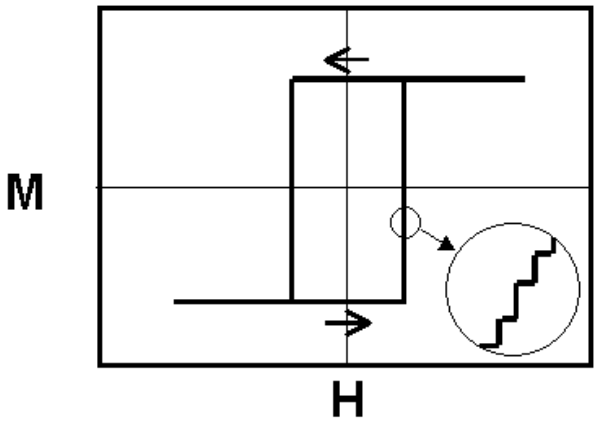

Figure 3.2: Schematic hysteresis loop taken with the field applied along the magnetic easy axis. One part is enlarged, showing that the magnetization reversal is taking place by a step-by-step motion of the magnetic domain wall.

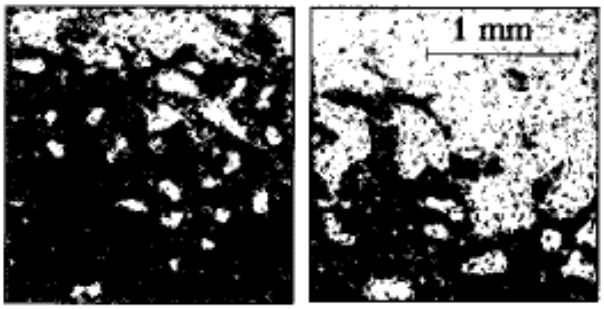

Figure 3.3: Propagation of magnetic domain walls in a 7 ML Fe film on Cu(001) in 15 seconds from the left to the right, obtained by Kerr microscopy [11]. $\mu_0 H_C$ of this film was 3.5 mT. The amplitude of the applied field was 0.82 mT.

where H is the magnetic field. The Barkhausen volume, V_B, is generally the smallest volume in which the magnetization reversed by one wall jump. The energy barrier, E_P, is the energy blocking or hindering the wall propagation. v_0 is in general the Barkhausen length ($=\sqrt[3]{V_B}$) divided by a time constant, τ. In Ref. [10], 10^9 s is used for τ, and 10^{10} s in Ref. [9]. In this report, the former will be used.

Thermally activated magnetic domain wall propagation in magnetic ultrathin films was carefully investigated with relation to surface morphology by magnetic after effect measurements in Ref. [11], and one of the examples is shown in Fig. 3.3. The sample was 7 atomic monolayer (ML) Fe a on Cu(001) clean surface, deposited in ultrahigh vacuum at room temperature. The out-of-plane easy axis was confirmed by the MOKE experiment. The film was initially magnetically saturated along the z axis, then a negative field 0.82 mT was applied to reverse the magnetization, which was smaller than $\mu_0 H_C$ (= 3.5 mT). Magnetic domain structures (left and right images in Fig. 3.3) were imaged by Kerr microscopy at 5 and 20 seconds after reversing the field, respectively. The white domains got bigger during the field. The estimated speed of wall propagation was about 10 m/s, and E_P was also obtained using Eq. (3.1). In the case of thin films, V_B can be a product of the size of surface terraces and film thickness, and E_p is the energy barrier that hinders wall propagation at the terrace edge. A larger thermal energy is needed for a wall overcome a larger barrier. Interestingly in Ref. [11], the distance of Barkhausen jumps is similar to the atomic terrace size of the Cu(001) clean surface, but much bigger than the size of Fe islands (20 - 40 nm).

Since the magnetization reversal by domain nucleation is also a thermally activated process, the domain nucleation probability, R, is presented in a similar way to the velocity of wall propagation,

$$\mathrm{R} = \frac{1}{\tau} \exp\left(\frac{\mu_0 M_S H \mathrm{V_N} - \mathrm{E_N}}{k_B T}\right). \tag{3.2}$$

In Ref. [9] for a GdFe alloy, the Barkhausen volume for domain nucleation, V_N, was found to be

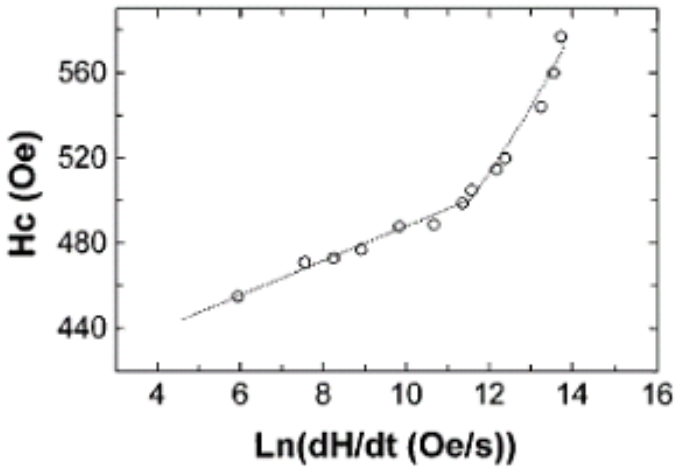

Figure 3.4: H_C vs. ln(dH/dt) curve obtained for a Au/0.8 nm Cu/Au sandwich system at room temperature. The dashed line is a guide to the eyes [42].

the same as V_p. In general, the barrier energy for nucleation, E_N, is larger than E_p, like it was found on this alloy system.

The magnetization reversal processes, magnetic domain nucleation and wall motion, are easily identified by H_C vs. ln(dH/dt) experiments [10, 42, 46–48]. An H_C vs. ln(dH/dt) curve from Ref. [42] is shown in Fig. 3.4. This curve was obtained for a Au/0.8 nm Cu/Au sandwich system at room temperature. When the sweep rate of the applied field is below 16 T/s (at the kink in Fig. 3.4), the wall propagation is dominating the reversal. Above that, mainly nucleation takes place.

Up to here, thermally activated magnetization reversal processes have been discussed. In the next section, the viscous wall motion is expressed, in which the speed of magnetic domain wall motion increases linearly as a function of the amplitude of H, when H is higher than H_{Crit}.

3.2 Viscous wall motion

In this section, the viscous wall motion, in which the wall velocity is proportional to the amplitude of applied field, will be interpreted. This is directly derived from the Landau-Lifshitz-Gilbert (LLG) equation of motion [13] in the case of a one-dimensional domain wall in a uniaxial anisotropy system, e.g., a Bloch wall in an FM film with an out-of-plane easy axis of magnetization.

Quantum mechanically, we have to consider the motion of a free spin, $\vec{S}$, in a time varying magnetic flux density, $\vec{B}(t)$, to which the magnetic moment $\gamma\vec{S}$ couples, where γ is the gyromagnetic ratio expressed in Section 3.2.1, can be described with the following Hamilton operator,

$$H = -\gamma\,\vec{S}\cdot\vec{B}(t). \tag{3.3}$$

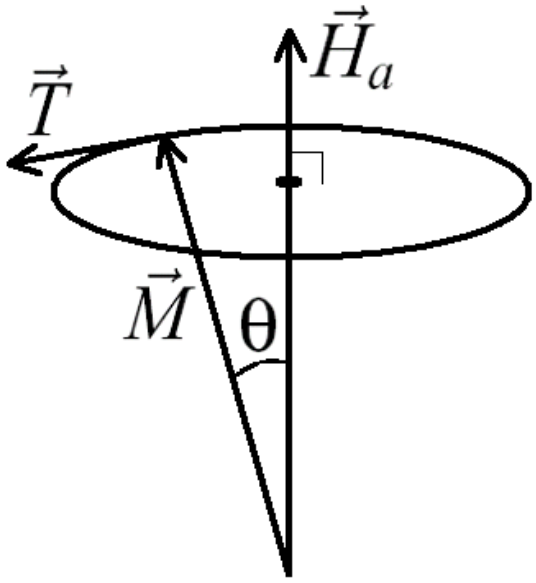

Figure 3.5: Torque, $\vec{T}$, on magnetization, $\vec{M}$, by an applied field, $\vec{H}_a$.

Then, the angular momentum is written as,

$$\frac{d\vec{S}}{dt} = \frac{1}{i\hbar}[\vec{S}, H] = \gamma\vec{S} \times \vec{B}. \tag{3.4}$$

The right hand side is the torque on the magnetic moment $\vec{S}$ in the magnetic field $\vec{B}$. The above equation can be rewritten by changing $\vec{S}$ to a magnetic dipole, $\vec{M}$,

$$\frac{d}{dt}\vec{M}(t) = \gamma[\vec{M}(t) \times \vec{B}(t)]. \tag{3.5}$$

And, with $\vec{B}$ is $\mu_0\vec{H}$ in vacuum,

$$\frac{d}{dt}\vec{M}(t) = -\gamma\mu_0[\vec{M}(t) \times \vec{H}(t)] \tag{3.6}$$

This formula is simplified and the basic equation of motion is written as,

$$-\frac{\dot{M}}{\gamma} = \mu_0\vec{M} \times \vec{H}_a. \tag{3.7}$$

The right hand side gives the torque, $\vec{T}$, acting on the magnetic dipole by the applied field, $\vec{H}_a$ (Fig. 3.5). The dipole precesses around $\vec{H}_a$ with a certain angle θ.

The precessional motion of magnetic dipoles in a magnetic material is not only driven by the Zeeman energy, but also by anisotropy, exchange and demagnetizing energies. Then Eq. 3.7 should be written with the effective field, H_{eff},

$$-\frac{\dot{M}}{\gamma} = \mu_0\vec{M} \times \vec{H_{eff}}, \tag{3.8}$$

where $\vec{H}_{eff}$ depends on the direction of $\vec{M}$. By introducing the damping, H_{eff} turns to be

$$\mu_0 \vec{H_{eff}} = -\frac{\partial w}{\partial \vec{M}} - \frac{\alpha \dot{\vec{M}}}{\gamma M}, \tag{3.9}$$

where w is energy volume density (dimension: J/m^3), including the Zeeman, anisotropy and exchange energies, and α the damping constant. Then the LLG equation of motion is

$$\dot{\vec{M}} = \gamma \vec{M} \times \frac{\partial w}{\partial \vec{M}} + \frac{\alpha \dot{\vec{M}} \times \vec{M}}{M}. \tag{3.10}$$

The first term on the right hand side is a stationary precession term. If there is no damping, i.e., $\mu_0 H_{eff}$ = –∂w/$\partial \vec{M}$, $\dot{\vec{M}}$ is always normal to the plane of $\vec{M}$ and $\vec{H}_{eff}$. This means that the spin precesses around the field direction in a cone, with θ remaining constant. This kind of precession is called "Larmor precession". This angular frequency, ω, is

$$\omega = \mu_0 \gamma H_{eff}. \tag{3.11}$$

Another feature of this behavior is that the static energy $-\mu_0 \vec{M} \cdot \vec{H_{eff}}$ does not change, and hence the motion is a conservative precession. The second term in Eq. 3.10 presents the process of damping, hence the energy is not conserved. By damping, the precessing moment loses energy and approaches to its static equilibrium direction along H_{eff}.

For the motion of a one-dimensional Bloch wall by a sufficiently high external field, the propagation speed of domain walls depends on the rate of energy dissipation by damping, the so called viscous wall motion. The energy dissipation density can be written,

$$\dot{w} = (\partial w/\partial \theta)\dot{\theta} + (\partial w/\partial \phi)\dot{\phi}, \tag{3.12}$$

where θ and ϕ are the angles in the y-z plane and in the x-z plane (see the coordinate system in Fig. 2.1), respectively. Then the LLG equation in polar and azimuthal components becomes

$$\dot{\theta} = -\frac{\gamma}{M}\frac{\partial w}{\partial \phi} sin\theta - \alpha \dot{\phi} sin\theta \tag{3.13}$$

$$\dot{\phi} sin\theta = \frac{\gamma}{M}\frac{\partial w}{\partial \theta} + \alpha \dot{\theta} \tag{3.14}$$

Solving the two equations above for δw/$\delta\phi$ and δw/$\delta\theta$, and substituting them into Eq. 3.12, one finds

$$\dot{w} = -\frac{\alpha}{\gamma M}\dot{\vec{M}}^2 = -\frac{M\alpha}{\gamma}(\dot{\theta}^2 + \dot{\phi}^2 sin^2\theta) \tag{3.15}$$

$$= \frac{M}{\gamma}[(\dot{\phi} sin\theta - \alpha\dot{\theta})\delta q - (-\theta sin\theta - \alpha\dot{\phi} sin^2\theta)\delta\phi]. \tag{3.16}$$

Integrating $\dot{w}$ along the y axis gives the corresponding differential in wall energy, $d\gamma_{DW}$,

$$d\gamma_{DW} = \frac{2M}{\gamma}[(-\dot{\phi} - \frac{\alpha\dot{q}}{\Delta})dq + (\dot{q} - \alpha\Delta\dot{\phi})d\phi], \tag{3.17}$$

where q and Δ represent the wall position with respect to the x axis and the wall width parameter, respectively. Eq. 3.17 is equivalent to the pair of partial differential equations

$$\frac{\partial\gamma_{DW}}{\partial\phi} = \frac{2M}{\gamma}(\dot{q} - \alpha\Delta\dot{\phi}), \tag{3.18}$$

$$\frac{\partial\gamma_{DW}}{\partial q} = -\frac{2M}{\gamma}(\phi - \frac{\alpha/rm\dot{q}}{\Delta}). \tag{3.19}$$

When a wall moves at some velocity $\dot{q}$ in a net uniform drive field H, the rate of Zeeman energy gained per unit area is

$$\dot{\gamma}_{DW} = -2\mu_0 MH\dot{q} \tag{3.20}$$

This energy gain must, according to energy conservation, be either stored in the intrinsic wall energy or else dissipate to the lattice by viscous damping. Integrate Eq. 3.20 over all space of ($\frac{\partial\gamma_{DW}}{\partial q}$ $\dot{q}$ + $\frac{\partial\gamma_{DW}}{\partial\phi}$ $\dot{\phi}$), which, using Eqs. 3.18 and 3.19,

$$\dot{\gamma}_{DW} = -\frac{2M\alpha}{\gamma}[\frac{\dot{q}^2}{\Delta} + \Delta\dot{\phi}^2] \tag{3.21}$$

This expression gives the dissipation function for wall motion. From Eq. 3.20 and Eq. 3.21, one gets,

$$\dot{q} = \frac{\alpha\Delta}{\gamma\,\mu_0\,\mathrm{H}}[\Delta^{-2}\dot{q}^2 + \dot{\phi}^2]. \tag{3.22}$$

If one supposes that $\dot{\phi}$ = 0, namely, the wall is always purely Bloch type, the velocity of wall motion, $\dot{q}$, will be

$$\dot{q} = \mathrm{v} = \frac{\gamma\Delta}{\alpha}\mathrm{H} \tag{3.23}$$

where an approximation $\langle\dot{q}^2\rangle$ = $\langle\dot{q}\rangle^2$ is used. Here the linear dependence of the domain wall velocity on the magnetic field is derived. The coefficient ($\gamma\Delta/\alpha$) is call the mobility of wall motion.

3.2.1 Gyromagnetic ratio

The gyromagnetic ratio $-\gamma$ is the ratio of the atomic magnetic moment $-g\mu_B J$ to the atomic angular momentum $\bar{h}J$, where J is the total moment, a sum of spin and orbital moments. The constant γ related to an effective dimensionless g-factor by the formula

$$\gamma = g\mu_B/\bar{h}, \tag{3.24}$$

where μ_B is the Bohr magneton,

$$\mu_B = e\bar{h}/(2m_e) = 9.27410 \times 10^{-24}\ \mathrm{J/T}. \tag{3.25}$$

where $\bar{h}$ = 1.05459 $\times$ 10^{-34} J s is Planck's constant divided by 2π, and e the electron charge (= 1.60218 $\times$ 10^{-19} C) and m_e the electron effective mass (= 9.10938 $\times$ 10^{-31} kg). For a free electron in a solid with spin but no orbital motion, the g-factor is 2.0023 and γ is 1.79 $\times$ 10^{11} (T s)$^{-1}$. These values can be used for itinerant 3d electrons in 3d transition metals.

3.3 Walker limit field

It was suggested in the above section that the wall velocity increases linearly with the field within a certain range. However, the velocity saturates at some effective field, the so called Walker limit

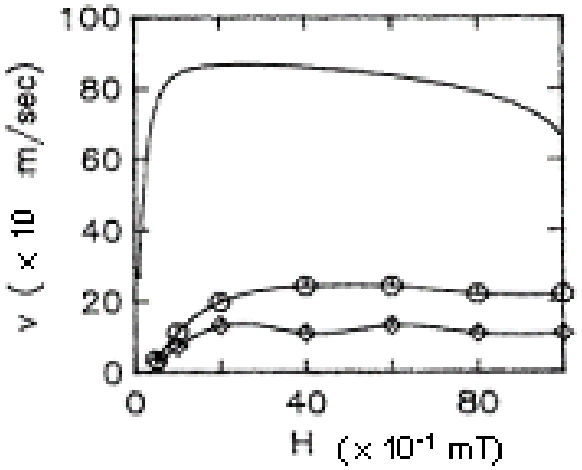

Figure 3.6: Domain wall velocity along the easy axis in FeNi vs. applied field. The solid line is the rigorous one-dimensional analytic solution calculated by Schryer and Walker [20], and the circles and diamonds are for 1000 *Å* and 500 *Å* thick films calculated by Yuan *et. al*. [21].

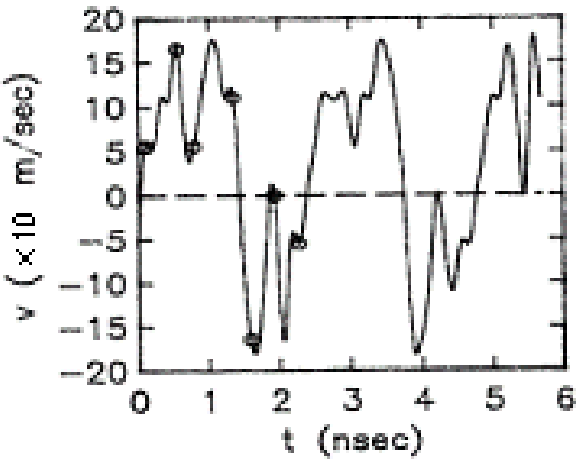

Figure 3.7: Simulation of wall velocity vs. time for a 500 *Å* thick FeNi film [21]. The applied field was 8.0 mT.

field, expressed as [20]

$$H_{Walker} = \frac{1}{2}\alpha M_S. \tag{3.26}$$

Above this field, the velocity may fluctuate or even oscillate, due to the fact that the spin structure inside the domain wall is varied by a high magnitude of the field. A simple explanation ca be given for a Bloch wall in a thin film with an out-of-plane anisotropy (Fig. 2.1 (a)), and with the applied field along the easy axis [21]. When the applied field exceeds H_{Walker}, spins inside the Bloch wall rotate also around the field axis. As a result, the wall involves also in-plane component, namely, the wall involves the Néel type wall. Two senses of spin precession, in the wall plane and in the film plane, co-exist. The harmony of these two precessional motions causes the oscillation of the wall velocity either as a function of time (Fig. 3.6) or as a function of field (Fig. 3.7).

In Fig. 3.6, the domain wall velocity vs. applied field is shown for 500 $\AA$ (diamonds) and 1000 $\AA$ (circles) thick FeNi films and a 1D analytic solution (solid curve) [21]. For a 500 $\AA$ thick FeNi film, a typical velocity evolution under high field (8 mT) as a function of time is shown in Fig. 3.7. The oscillatory transition between Bloch and Néel wall manifests itself by the oscillation of wall velocity (Fig. 3.7), since the masses and viscosities of these walls are very different from each other [21].

Oscillatory motion of a transverse head-on Néel wall in a narrow stripe of FeNi (5 nm-thick, 1250 nm-long and various widths from 5 to 35 nm) has been simulated analytically and fully computationally [22]. There it was mentioned that if the external field along the longitudinal direction of the stripe is sufficiently strong, the spins in the wall precess also around the field axis. Then the spins have also a magnetization component normal to the film plane, such that the spins precess also around the z axis by the demagnetizing field. The energy loss for this damping lowers the wall velocity. It was mentioned in that article that H_{Walker} is the field which can point spins normal to the film plane. It was also observed there that H_{Walker} depended on the ratio between width and thickness of the stripe, which reflects the ratio between out-of-plane and in-plane stray field energies under the external field.